Photocatalysis

International Edition: DOI: 10.1002/anie.201502686
German Edition: DOI: 10.1002/ange.201502686

Efficient Visible-Light-Driven Z-Scheme Overall Water Splitting Using a $MgTa_2O_{6-x}N_y$/TaON Heterostructure Photocatalyst for H_2 Evolution**

Shanshan Chen, Yu Qi, Takashi Hisatomi, Qian Ding, Tomohiro Asai, Zheng Li, Su Su Khine Ma, Fuxiang Zhang, Kazunari Domen, and Can Li**

Abstract: *An (oxy)nitride-based heterostructure for powdered Z-scheme overall water splitting is presented. Compared with the single $MgTa_2O_{6-x}N_y$ or TaON photocatalyst, a $MgTa_2O_{6-x}N_y$/TaON heterostructure fabricated by a simple one-pot nitridation route was demonstrated to effectively suppress the recombination of carriers by efficient spatial charge separation and decreased defect density. By employing Pt-loaded $MgTa_2O_{6-x}N_y$/TaON as a H_2-evolving photocatalyst, a Z-scheme overall water splitting system with an apparent quantum efficiency (AQE) of 6.8% at 420 nm was constructed (PtO_x-WO_3 and IO_3^-/I^- pairs were used as an O_2-evolving photocatalyst and a redox mediator, respectively), the activity of which is circa 7 or 360 times of that using Pt-TaON or Pt-$MgTa_2O_{6-x}N_y$ as a H_2-evolving photocatalyst, respectively. To the best of our knowledge, this is the highest AQE among the powdered Z-scheme overall water splitting systems ever reported.*

Inspired by natural photosynthesis, semiconductor-based Z-scheme overall water splitting for hydrogen production has attracted extensive attention.[1] To date, many (oxy)nitride semiconductors with wide visible-light utilization have been studied as proton-reduction photocatalysts in the Z-scheme overall water splitting system, but the poor separation of photogenerated carriers severely restricts the overall photocatalytic efficiency.[1c,2] Some strategies, such as surface modification and construction of solid solution, have been introduced to inhibit the recombination of carriers by reducing the defect density of the (oxy)nitrides.[2b–d,3] The highest apparent quantum efficiency (AQE = 6.3% at 420 nm) ever reported for Z-scheme overall water splitting is using Pt-ZrO_2/TaON and PtO_x-WO_3 as a H_2-evolving photocatalyst and an O_2-evolving photocatalyst, respectively.[2c] However, the current efficiency of the photocatalytic water reduction is still much lower than that of water oxidation on PtO_x-WO_3 (about 20% at 420 nm) in the Z-scheme system with IO_3^-/I^- shuttle ions.[4] Thus, the development of an effective strategy to improve the H_2-evolving rate, especially to enhance the separation of photogenerated carries, is extremely desirable.

Besides those reported strategies of surface modification and solid solution, the semiconductor–semiconductor heterostructure has been known to effectively promote the interfacial charge transfer via the heterojunction.[5] To date, most heterostructures have been constructed based on UV-responsive oxides by in situ growth of one material onto the other with an annealing treatment in air.[6] However, the (oxy)nitride semiconductors are thermally unstable in air, and their synthesis commonly involves a high temperature and requires an accompanying reducing agent, namely ammonia. As a result, it still remains challenging to fabricate the heterostructure between oxynitride and oxide without deteriorating their structures.[5g]

Herein we present the preparation of a $MgTa_2O_{6-x}N_y$/TaON heterostructure with an emphasis on one-pot nitridation from $MgTa_2O_6/Ta_2O_5$ precursor under an ammonia flow free of annealing treatment in air. The as-fabricated $MgTa_2O_{6-x}N_y$/TaON heterostructure can effectively suppress the recombination of carriers and enhance the H_2-evolving rate. Together with PtO_x-WO_3 as an O_2-evolving photocatalyst, and IO_3^-/I^- pair as a redox mediator, we finally achieved an AQE of 6.8% at 420 nm for Z-scheme overall water splitting, which is the highest value among the powdered Z-scheme systems ever reported.

The heterostructures with different molar ratios of Mg/Ta were prepared by one-pot nitridation of $MgTa_2O_6/Ta_2O_5$ precursor under an ammonia flow at 1123 K for 15 h. The as-obtained samples are denoted as $MgTa_2O_{6-x}N_y$/TaON(n), where "n" stands for the molar ratio of Mg/Ta. Single phase of TaON or $MgTa_2O_{6-x}N_y$ was similarly prepared by using Ta_2O_5 or $MgTa_2O_6$ as precursor. Both of them are visible-light-active for water oxidation and proton-reduction reactions.[7] For comparison, TaON and $MgTa_2O_{6-x}N_y$ with Mg/Ta molar ratio

[*] S. Chen, Y. Qi, Q. Ding, Z. Li, Prof. F. Zhang, Prof. C. Li
State Key Laboratory of Catalysis, iChEM, Dalian Institute of Chemical Physics, Chinese Academy of Sciences
Dalian National Laboratory for Clean Energy
Dalian, 116023 (China)
E-mail: fxzhang@dicp.ac.cn
canli@dicp.ac.cn

S. Chen, Y. Qi, Q. Ding, Z. Li
University of Chinese Academy of Sciences
Beijing 100049 (China)

Dr. T. Hisatomi, T. Asai, Dr. S. Ma, Prof. K. Domen
Department of Chemical System Engineering
School of Engineering, The University of Tokyo
7-3-1 Hongo, Bunkyo-ku, Tokyo 113-8656 (Japan)

[**] This work was supported by the Basic Research Program of China (973 Program: 2014CB239403), Natural Science Foundation of China (No. 21361140346, 21373210), and a Grant-in-Aid for specially promoted research (No. 23000009) of the Japan Society for the Promotion of Science (JSPS). F.Z. thanks the support from the "Hundred Talents Program" of CAS.

Supporting information for this article is available on the WWW under http://dx.doi.org/10.1002/anie.201502686.

of 0.2 are mechanically mixed and denoted as $MgTa_2O_{6-x}N_y$/TaON(0.2)-mix. Details of materials preparation is given in the Supporting Information; XRD patterns of the typical nitrided samples as well as the corresponding precursors are shown in Figure S1. Compared with the single phase of TaON or $MgTa_2O_{6-x}N_y$, the diffraction peaks of the heterostructured or mixed sample are not obviously shifted.

The photocatalytic performance of Z-scheme overall water splitting is dependent on the amount of deposited platinum and the molar ratio of Mg/Ta. The platinum loading amounts for the H_2 and O_2 evolution photocatalysts are optimized to be 0.4 wt% and 0.45 wt%, respectively (Supporting Information, Figure S2). Based on this condition, the activity curve as a function of Mg/Ta molar ratio exhibits a volcano type with an optimized value of about 0.2, and the molar ratios of H_2/O_2 evolved are close to 2:1 (Supporting Information, Figure S3). The optimized photocatalytic overall water splitting performance using Pt-$MgTa_2O_{6-x}N_y$/TaON-(0.2) as a H_2-evolving photocatalyst is about 7, or 360 times that using Pt-TaON or Pt-$MgTa_2O_{6-x}N_y$, respectively, demonstrating the excellent promotion effect of the heterostructure. No obvious deactivation was found in the tested period (Supporting Information, Figure S4). The influence of possible residual SO_4^{2-} on the photocatalytic performance was also ruled out by a comparative experiment. The typical results are summarized in Table 1. It is interesting to note that using the

Table 1: Photocatalytic performance of typical photocatalysts with different surface areas under visible-light irradiation ($\lambda \geq 420$ nm).

Entry	Photocatalyst[a]	Surface area [$m^2 g^{-1}$]	Gas evolution rates [$\mu mol\, h^{-1}$][b] H_2	O_2
1	$MgTa_2O_{6-x}N_y$	1.1	0.3	1.3
2	TaON	8.5	15.6	7.5
3	$MgTa_2O_{6-x}N_y$/TaON(0.2)-mix	6.7	23.5	12.2
4	$MgTa_2O_{6-x}N_y$/TaON(0.2)	6.9	108.3	55.3

[a] All photocatalysts were loaded with 0.4 wt% Pt by impregnation and subsequent H_2 reduction method. [b] Reaction conditions: 75 mg H_2 evolution photocatalyst and 150 mg 0.45 wt% PtO_x-WO_3 photocatalyst; 150 mL aqueous NaI solution (1.0 mM); Pyrex top-irradiation type; 300 W xenon lamp.

mechanically mixed Pt-$MgTa_2O_{6-x}N_y$/TaON(0.2)-mix sample as the H_2-evolving photocatalyst (entry 3), the gas evolution rates are also promoted but not as effectively as that using the heterostructured sample (entry 4). Correspondingly, the AQE of Z-scheme overall water splitting was measured (Supporting Information, Table S1), and the optimal AQE of 6.8% at 420 nm was finally achieved.

To insight the promotion effect of the heterostructure on the photocatalytic performance, the physical properties of typical samples in Table 1 were first characterized by FESEM. As shown in Figure 1, the surface of TaON sample is rough and porous (Figure 1 a), while that of $MgTa_2O_{6-x}N_y$ sample is relatively smooth without porosity (Figure 1 b). Therefore, the substances of TaON and $MgTa_2O_{6-x}N_y$ can be identified simply by the surface roughness, which is further verified by the EDX results (Supporting Information, Figure S5). The

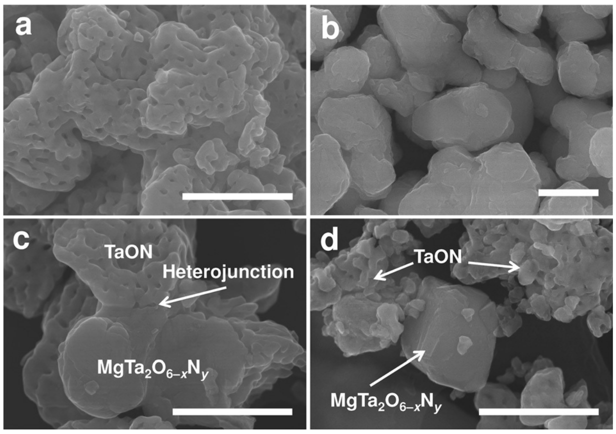

Figure 1. Representative FESEM images of typical samples: a) TaON, b) $MgTa_2O_{6-x}N_y$, c) $MgTa_2O_{6-x}N_y$/TaON(0.2), and d) $MgTa_2O_{6-x}N_y$/TaON(0.2)-mix. Scale bars: 500 nm.

typical morphologies of TaON and $MgTa_2O_{6-x}N_y$ are both observed for the heterostructured (Figure 1 c) and mixed samples (Figure 1 d), but their interfacial contact is remarkably different. Compared with the mixed sample, the interfacial contact between $MgTa_2O_{6-x}N_y$ and TaON on the heterostructured sample is more intimate and abundant. Furthermore, according to the absorption background of UV/Vis DRS of typical samples with different molar ratios of Mg/Ta (Supporting Information, Figure S6), the defect density on the heterostructured sample is relatively decreased.

Secondly, the time-resolved infrared spectra (TRIR) of the typical samples (Figure 2 A) reveals that the mixed or heterstructured sample exhibits a prolonged lifetime of carriers with respect to the single component of samples. Since a simple mechanical mixing treatment does not obviously change their basic physical structures such as particle size (Figure 1), surface area (Table 1), and defect density (Supporting Information, Figure S6), the prolonged lifetime of carriers on the mixed sample is proposed to originate from the spatial charge transfer between the semiconductors via the particle–particle collision. Compared with the mechanically mixed sample, the lifetime of carriers on the heterostructured sample is much longer, originating from its more intimate interfacial contact and decreased defect density, both of which are favorable for the inhibition of carriers recombination.[8] The prolonged lifetime of carriers is expected to be responsible for the enhancement of photocatalytic activity.[9]

Furthermore, dependence of the H_2 evolution rate on the wavelength of the irradiation light was examined to discuss the promotion effect of the heterostructure. As shown in Figure 2 B, the trends of H_2 evolution rates on the tested photocatalysts (Pt-TaON and Pt-$MgTa_2O_{6-x}N_y$/TaON(0.2)) are generally consistent with their UV/Vis DRS, indicating the photocatalytic performances are driven by the incident light. On the other hand, the photocatalytic H_2 evolution rates on the heterostructured sample are always much higher than those on the Pt-TaON sample under the same irradiation wavelength. Furthermore, once the photocatalysts are irradiated with the cutoff wavelength of 520 nm ($\lambda \geq 520$ nm) to just

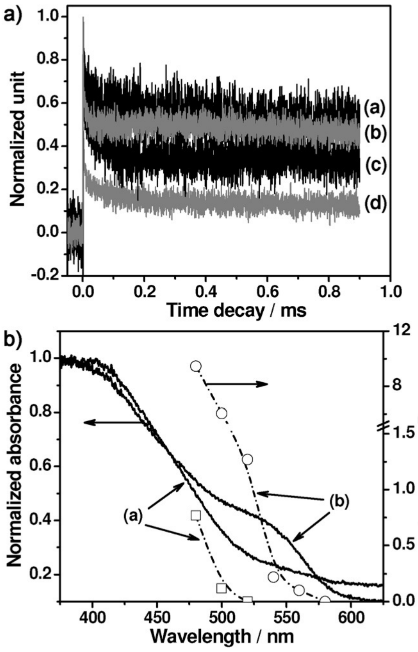

Figure 2. A) Normalized transient absorption profiles of the representative samples in a vacuum: a) Pt-$MgTa_2O_{6-x}N_y$/TaON(0.2), b) Pt-$MgTa_2O_{6-x}N_y$/TaON(0.2)-mix, c) Pt-TaON, d) Pt-$MgTa_2O_{6-x}N_y$. The pulse laser at 355 nm was used to excite the samples for the IR tests. The cocatalyst of Pt with a loading amount of 0.4 wt% was deposited by impregnation and subsequent H_2 reduction method. B) Dependence of the H_2 evolution rate on the cutoff wavelength of incident light (dotted lines) and the normalized UV/Vis DRS of a) TaON and b) $MgTa_2O_{6-x}N_y$/TaON(0.2) samples (solid lines). Reaction conditions: 0.15 g photocatalyst loaded with 0.4 wt% Pt cocatalyst; aqueous 20 v% CH_3OH solution buffered with 0.15 g La_2O_3 (150 mL); Pyrex top-irradiation type; 300 W xenon lamp.

excite the $MgTa_2O_{6-x}N_y$ component, H_2 can only be detected on the heterostructured sample instead of TaON within the experimental region, and the corresponding activity of Pt-$MgTa_2O_{6-x}N_y$/TaON(0.2) is even higher than that of Pt-$MgTa_2O_{6-x}N_y$ photocatalyst under visible light irradiation ($\lambda \geq 420$ nm). These results together reveal that an efficient spatial charge transfer between TaON and $MgTa_2O_{6-x}N_y$ exists in the heterostructured photocatalyst.

To experimentally test the spatial transfer of photogenerated electrons on the heterostructured sample, photoreduction deposition of platinum ions under visible light irradiation ($\lambda \geq 420$ nm) was thus carried out in the presence of methanol.[10] As shown in Figure 3 a,b, photoreduced Pt nanoparticles are mainly deposited on the surface of porous TaON, instead of the smooth surface of $MgTa_2O_{6-x}N_y$, demonstrating an accumulation of photogenerated electrons on the TaON surface. The incapability of photoreducing the $[PtCl_6]^{2-}$ ion on the $MgTa_2O_{6-x}N_y$ surface is ruled out by the corresponding blank experiment (Supporting Information, Figure S7). Moreover, the random deposition of Pt nanoparticles on the surfaces of both TaON and $MgTa_2O_{6-x}N_y$ by conventional impregnation and subsequent H_2 reduction method (Supporting Information, Figure S8) also excludes the possible selective adsorption of $[PtCl_6]^{2-}$ ion on these different surfaces. Thus, it renders us to reasonably ascribe the selective photodeposition of platinum nanoparticles (Figure 3 a,b) to an accumulation of photogenerated electrons on the surface of TaON, confirming the spatial transfer of the photoinduced electrons from $MgTa_2O_{6-x}N_y$ to TaON.

The thermodynamic feasibility of spatial charge transfer between TaON and $MgTa_2O_{6-x}N_y$ is confirmed by their relative band positions, which were characterized by Mott–Schottky (M-S) plots, X-ray photoelectronic spectra (XPS), and UV/Vis DRS. According to the M-S plots (Supporting Information, Figure S9 a), the flat-band potentials of $MgTa_2O_{6-x}N_y$ and TaON are fitted to be about -0.38 V and -0.31 V versus NHE (pH 8.5), respectively. The valence band (VB) maximum of TaON is more positive about 0.32 eV than that of $MgTa_2O_{6-x}N_y$ based on the total densities of states of XPS VB spectra (Supporting Information, Figure S9 b). Together with their band gaps, a detailed band-structure diagram of $MgTa_2O_{6-x}N_y$/TaON heterostructure is thus proposed in Figure 3 c, in which the relative potential difference of energy levels between $MgTa_2O_{6-x}N_y$ and TaON belongs to the typical type II heterojunction with the thermodynamical feasibility of the spatial transfer of photogenerated carriers.

It should be pointed out that the heterostructure formed via the one-pot nitridation route introduced herein does not need any additional annealing treatments in air, so it can effectively avoid the possible deterioration of the components. Another advantage is that the nitridation at the high temperature of 1123 K is in favor of making a strong interaction at the interface, leading to the formation of an intimate interfacial contact (Figure 1 c, Figure 3 a,b) and the passivation of interfacial dangling bonds causing decreased defect density (Supporting Information, Figure S6). Both of them integrally contributes to the remarkably enhanced lifetime of carriers as well as the improved photocatalytic performance. Compared with the previous surface passivation

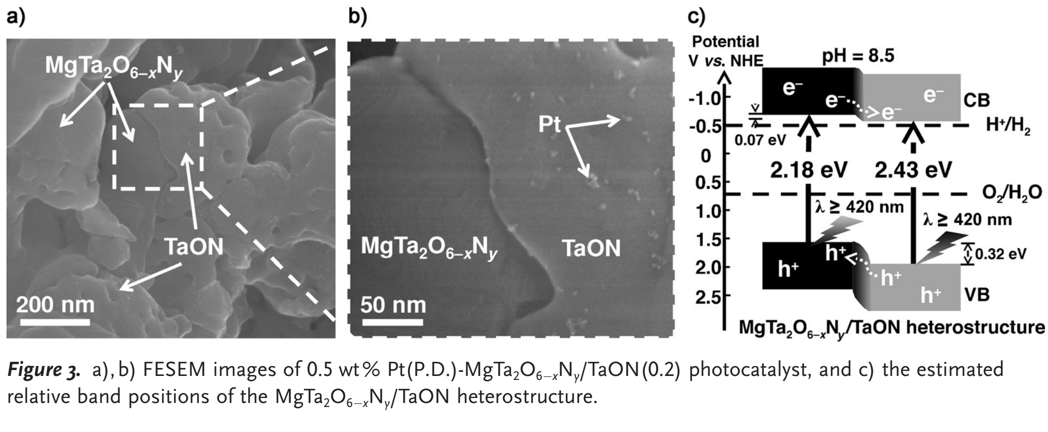

Figure 3. a), b) FESEM images of 0.5 wt% Pt(P.D.)-$MgTa_2O_{6-x}N_y$/TaON(0.2) photocatalyst, and c) the estimated relative band positions of the $MgTa_2O_{6-x}N_y$/TaON heterostructure.

modification of ZrO_2 on the TaON sample,[2b,c] the as-fabricated $MgTa_2O_{6-x}N_y$/TaON heterostructure herein not only reduces the defect density, but also favors the spatial charge separation by the heterojunction. Moreover, extended visible light utilization can be anticipated for the heterostructure strategy. Accordingly, it is expected to be an alternative promising strategy for (oxy)nitrides to achieve enhanced solar energy conversion efficiency.

In summary, a novel $MgTa_2O_{6-x}N_y$/TaON heterostructure was fabricated by a one-pot nitridation strategy to inhibit the recombination of carriers. Employing it as a H_2-evolving photocatalyst, we achieve an AQE of 6.8% at 420 nm, which is a new benchmark for visible-light-driven photocatalytic Z-scheme overall water splitting reaction using powdered photocatalysts. The promotion of photocatalytic performance is mainly ascribed to the enhanced charge separation originating from the well-matched heterostructure and the decreased defect density. To the best of our knowledge, this is the first successful heterostructure based on an oxynitride and a nitrogen-doped oxide for particulate visible-light-driven Z-scheme overall water splitting. There are many (oxy)nitrides and nitrogen-doped oxides with wide visible light utilization and different structures of energy levels,[11] so the one-pot nitridation strategy is promising for them to construct other heterostructured photocatalysts for efficient solar energy conversion.

Keywords: heterostructures · hydrogen · overall water splitting · oxynitrides · photocatalysis

How to cite: *Angew. Chem. Int. Ed.* **2015**, *54*, 8498–8501
Angew. Chem. **2015**, *127*, 8618–8621

[1] a) A. J. Bard, *J. Photochem.* **1979**, *10*, 59–75; b) K. Sayama, K. Mukasa, R. Abe, Y. Abe, H. Arakawa, *Chem. Commun.* **2001**, 2416–2417; c) R. Abe, *Bull. Chem. Soc. Jpn.* **2011**, *84*, 1000–1030; d) A. Kudo, *MRS Bull.* **2011**, *36*, 32–38; e) K. Maeda, *ACS Catal.* **2013**, *3*, 1486–1503.

[2] a) M. Higashi, R. Abe, K. Teramura, T. Takata, B. Ohtani, K. Domen, *Chem. Phys. Lett.* **2008**, *452*, 120–123; b) K. Maeda, H. Terashima, K. Kase, M. Higashi, M. Tabata, K. Domen, *Bull. Chem. Soc. Jpn.* **2008**, *81*, 927–937; c) K. Maeda, M. Higashi, D. L. Lu, R. Abe, K. Domen, *J. Am. Chem. Soc.* **2010**, *132*, 5858–5868; d) T. Matoba, K. Maeda, K. Domen, *Chem. Eur. J.* **2011**, *17*, 14731–14735; e) D. J. Martin, P. J. T. Reardon, S. J. A. Moniz, J. W. Tang, *J. Am. Chem. Soc.* **2014**, *136*, 12568–12571.

[3] K. Maeda, D. L. Lu, K. Domen, *ACS Catal.* **2013**, *3*, 1026–1033.

[4] Y. Miseki, S. Fujiyoshi, T. Gunjib, K. Sayama, *Catal. Sci. Technol.* **2013**, *3*, 1750–1756.

[5] a) J. S. Jang, H. G. Kim, J. S. Lee, *Catal. Today* **2012**, *185*, 270–277; b) X. Wang, Q. Xu, M. R. Li, S. Shen, X. L. Wang, Y. C. Wang, Z. C. Feng, J. Y. Shi, H. X. Han, C. Li, *Angew. Chem. Int. Ed.* **2012**, *51*, 13089–13092; *Angew. Chem.* **2012**, *124*, 13266–13269; c) E. S. Kim, N. Nishimura, G. Magesh, J. Y. Kim, J. W. Jang, H. Jun, J. Kubota, K. Domen, J. S. Lee, *J. Am. Chem. Soc.* **2013**, *135*, 5375–5383; d) R. Marschall, *Adv. Funct. Mater.* **2014**, *24*, 2421–2440; e) H. L. Wang, L. S. Zhang, Z. G. Chen, J. Q. Hu, S. J. Li, Z. H. Wang, J. S. Liu, X. C. Wang, *Chem. Soc. Rev.* **2014**, *43*, 5234–5244; f) Y. P. Yuan, L. W. Ruan, J. Barber, S. C. J. Loo, C. Xue, *Energy Environ. Sci.* **2014**, *7*, 3934–3951; g) H. Kim, D. Monllor-Satoca, W. Kim, W. Choi, *Energy Environ. Sci.* **2015**, *8*, 247–257.

[6] J. Zhang, Q. Xu, Z. C. Feng, M. R. Li, C. Li, *Angew. Chem. Int. Ed.* **2008**, *47*, 1766–1769; *Angew. Chem.* **2008**, *120*, 1790–1793.

[7] a) G. Hitoki, T. Takata, J. N. Kondo, M. Hara, H. Kobayashi, K. Domen, *Chem. Commun.* **2002**, 1698–1699; b) S. S. Chen, Y. Qi, G. J. Liu, J. X. Yang, F. X. Zhang, C. Li, *Chem. Commun.* **2014**, *50*, 14415–14417.

[8] a) X. P. Lin, F. Q. Huang, J. C. Xing, W. D. Wang, F. F. Xu, *Acta Mater.* **2008**, *56*, 2699–2705; b) F. X. Zhang, A. Yamakata, K. Maeda, Y. Moriya, T. Takata, J. Kubota, K. Teshima, S. Oishi, K. Domen, *J. Am. Chem. Soc.* **2012**, *134*, 8348–8351; c) S. S. Chen, S. Shen, G. J. Liu, Y. Qi, F. X. Zhang, C. Li, *Angew. Chem. Int. Ed.* **2015**, *54*, 3047–3051; *Angew. Chem.* **2015**, *127*, 3090–3094.

[9] a) A. Yamakata, T. Ishibashi, H. Onishi, *J. Phys. Chem. B* **2002**, *106*, 9122–9125; b) T. Chen, Z. C. Feng, G. P. Wu, J. Y. Shi, G. J. Ma, P. L. Ying, C. Li, *J. Phys. Chem. C* **2007**, *111*, 8005–8014.

[10] a) T. Ohno, K. Sarukawa, M. Matsumura, *New J. Chem.* **2002**, *26*, 1167–1170; b) R. G. Li, F. X. Zhang, D. E. Wang, J. X. Yang, M. R. Li, J. Zhu, X. Zhou, H. X. Han, C. Li, *Nat. Commun.* **2013**, *4*, 1432.

[11] a) S. S. Chen, J. X. Yang, C. M. Ding, R. G. Li, S. Q. Jin, D. E. Wang, H. X. Han, F. X. Zhang, C. Li, *J. Mater. Chem. A* **2013**, *1*, 5651–5659; b) T. Hisatomi, J. Kubota, K. Domen, *Chem. Soc. Rev.* **2014**, *43*, 7520–7535; c) X. Zong, L. Z. Wang, *J. Photochem. Photobiol. C* **2014**, *18*, 32–49.

Received: March 25, 2015
Revised: April 23, 2015
Published online: June 3, 2015